Zehra Ese*, Marcel Kressmann, Jakob Kreutner, Gregor Schaefers, Daniel Erni, and Waldemar Zylka

Influence of conventional and extended CT scale range on quantification of Hounsfield units of medical implants and metallic objects

Einfluss des konventionellen und erweiterten CT-Skalenbereiches auf die Quantifizierung von Hounsfield-Werten von medizinischen Implantaten und metallischen Objekten

https://doi.org/10.1515/teme-2017-0122
Received October 9, 2017; revised December 12, 2017; accepted February 21, 2018

Abstract: We report on the suitability of two different ranges of Hounsfield units (HU) in computed tomography (CT) for the quantification of metallic components of active implantable medical devices (AIMD). The conventional Hounsfield units (CHU) range, which is traditionally used in radiology, is well suited for tissue but suspected inappropriate for metallic materials. Precise HU values are notably beneficial in radiotherapy (RT) for accurate dose calculations, thus for the safety of patient carrying implants. Some of today's CT machines offers an extended Hounsfield units (EHU) range. This study presents CT acquisitions of a water phantom containing various metallic discs and an implantable-cardioverter defibrillator (IPG). We show that the comparison of HU values at EHU and CHU ranges clearly reveals the superiority and accuracy of EHU. Some geometrical discrepancies perpendicular to slices are observed. At EHU metal artifact reduction algorithms (MAR) underestimates HU values rendering MAR potentially inappropriate for RT.

Keywords: Hounsfield unit, computed tomography, medical implants, radiation therapy.

Zusammenfassung: Wir berichten über den Einfluss von zwei verschiedenen Skalenbereichen für Hounsfiled-Werte (HU) auf die Quantifizierung von metallischen Komponenten von aktiven medizinisch implantierbaren Medizinprodukten (AIMD) in der Computertompgraphie (CT). Der konventionelle Hounsfield-Wertebereich (CHU), welcher seine Anwendung in der traditionellen Radiologie findet, ist geeignet für Gewebe jedoch ungeeignet für metallische Materialien. Präzise HU-Werte sind besonders wichtig für eine akurate Dosis-Berechnung in der Strahlentherapie, insbesondere bei Patienten mit medizinischen Implantaten. Einige der heutigen CT-Systeme bieten einen erweiterten HU-Bereich (EHU). In dieser Arbeit werden CT-Aufnahmen von diversen metallischen Platten und einem Kardioverter-Defibrillator (ICD) im Wasserphantom präsentiert. Der Vergleich von HU-Werten bei EHU- und CHU-Bereichen zeigt eine deutlich höhere Genauigkeit im EHU-Bereich. Es werden einige geometrische Diskrepanzen senkrecht zu Schichtaufnahme beobachtet. Festgestellt wird, dass bei EHU-Metall-Artefakt-Reduktionsalgorithmen (MAR) HU-Werte unterschätzt werden, wodurch MAR für RT möglicherweise unangemessen ist.

Schlagwörter: Hounsfield-Werte, Computertomographie, Strahlentherapie.

PACS: 87.85.J-, 87.57.Q-, 87.56.bd, 87.55.dk

***Corresponding author: Zehra Ese,** MR:comp GmbH, Buschgrundstraße 23, 45894 Gelsenkirchen, Germany; and Laboratory for General and Theoretical Electrical Engineering (ATE), Faculty of Engineering, University of Duisburg-Essen, Bismarckstrasse 81, 47048 Duisburg, Germany; and Faculty of Electrical Engineering and Applied Natural Sciences, Westphalian University, Campus Gelsenkirchen, Neidenburger Strasse 43, 45897 Gelsenkirchen, Germany, e-mail: ese@mrcomp.com
Marcel Kressmann, MR:comp GmbH, Buschgrundstraße 23, 45894 Gelsenkirchen, Germany
Jakob Kreutner, Gregor Schaefers, MR:comp GmbH, Buschgrundstraße 23, 45894 Gelsenkirchen, Germany; and MRI-STaR – Magnetic Resonance Institute for Safety, Technology and Research GmbH, Buschgrundstraße 23, 45894 Gelsenkirchen, Germany
Daniel Erni, Laboratory for General and Theoretical Electrical Engineering (ATE), Faculty of Engineering, University of Duisburg-Essen and CENIDE – Center of Nanointegration Duisburg-Essen, Bismarckstrasse 81, 47048 Duisburg, Germany
Waldemar Zylka, Faculty of Electrical Engineering and Applied Natural Sciences, Westphalian University, Campus Gelsenkirchen, Neidenburger Strasse 43, 45897 Gelsenkirchen, Germany

1 Introduction

Due to the aging population the number of patients with AIMDs and the occurrence of malignancies, especially cancer, are rising steadily. According to a recent study 14.1 million new cancer cases appeared worldwide in 2016 and this number is expected to double by 2050 [1]. Half of all cancer patients is treated with RT at least once during the course of his or her disease [2]. Therefore, the probability of patients receiving RT due to malignancy while wearing an implant is increasing [3, 4, 5, 6, 7].

The goal of RT is to deliver a well-defined homogeneous radiation dose to a target volume (malignant tissue) while minimizing radiation to the surrounding healthy tissue and to nearby critical objects like AIMDs. However, the interactions of ionizing radiation and AIMDs and their meaning for RT are not well established yet. Especially, there are many concerns regarding the beam energy, dose and dose-rate limitations to the AIMD with respect to malfunction that may occur in these devices that could jeopardize patient safety. Nonetheless, many institutions refer to the 1994 report of the American Association of Physicist in Medicine (AAPM) task group no. 34 [8] about managing radiation oncology patients with implanted cardiac pacemakers, even though that report only focuses on pacemakers and does not consider other AIMDs. The main recommendations given by the AAPM are: (i) to avoid positioning the pacemaker in the direct beam and (ii) to limit the absorbed dose to the pacemaker to 2 Gy. Case reports show that, depending on the applied beam energy, IPG malfunctions can occur even bellow this threshold [4].

Since there are many conflicts regarding the handling of radiooncology patients with implants, many institutions use methods drawn from their experiences. In 2012, Hurkmans et al. [9] published guidelines for the management of patients with cardiac implantable electronic devices (CIED) in the Netherlands. They categorized patient examinations into different risk levels according to their implant dependency and the estimated radiation dose applied to the CIED depending on the tumor localization. Three dose-levels were evaluated: more than 10 Gy for tumors located at the upper zone of the neck and the thorax, 2 Gy to 10 Gy for tumors in the medium zone of the thorax as well as in the half-lower section of the head and less than 2 Gy for tumors in the rest of the body [9, 10]. In 2015, Gauter-Fleckenstein et al. [3] published new German guidelines for handling RT patients with CIEDs. These recommended guidelines were based on the suggestions by Hurkmans et al. [9] and reflect the patient risk according to the type of CIED, cardiac conditions and estimated radiation dose to the CIED. It was advised that the RT treatment planning should consider the CIED specifications as well as patient related characteristics. However, it is still difficult to precisely determine the dose to the AIMD during radiation exposure, since AIMDs are mostly not exposed by the direct beam.

It is well established that current RT treatment planning systems (TPS) are not able to model the out-of-field doses beyond the beam penumbra [10, 11]. The accuracy of dose calculations is known to decrease with increasing distance from the field edge. However, peripheral doses depend on beam energy, field size and distance from field edge and are commonly estimated based on previous publications [12]. RT TPS is commonly based on computed tomography (CT) data of the patient, which provide information about the geometry and localization of the tumor as well as the anatomy of the patient's body. In addition, tissue dependent radiodensity values, which are essential for accurate dose calculation in the TPS are derived from the CT data. Treatment planning calculations are based on the proper segmentation of the target structures and organs. The complexity of the geometry, tissue and materials in the segmented regions define the type of treatment and the beam energies to be used.

High-density materials frequently used in metallic implants can cause significant challenges in realizing an efficient treatment plan. For instance, image artefact are destroying object geometry, unknown radiodensity values cause their incorrect assignment and many other effects [13, 14, 15, 16]. In fact, in today's clinical RT practice, high-density regions are removed by assigning the HU value of water to the manually contoured region. To achieve appropriate dose calculation, the HU value of implant materials have to be determined. However, the majority of CT scanners are used in radiology and implements only a conventional CHU range which suffices to properly represent all different human body tissues. HU values of dense materials, e. g. metals, considerably exceed the maximum of CHU thus these materials are usually mapped to CHU's maximum [14].

In this study we investigate CT scanner HU values of metallic and electrical components of implants at the conventional CHU range and compare them to those at the extended EHU range. We research the suitability of CHU and EHU range for the representation of high-density implant materials which would allow to draw conclusions regarding the superiority of EHU in accurate dose calculations and increase patient safety in RT.

2 Material and methods

The Hounsfield scale is defined based on X-ray absorption coefficient of water μ(water). The HU value (also known as CT number) of a particular material with X-ray absorption coefficient μ is calculated by:

$$HU = 1000\,\text{HU}\frac{\mu - \mu(\text{water})}{\mu(\text{water})}. \quad (1)$$

Obviously, –1000 HU corresponds to air (μ(air) = 0) while 0 HU is assigned to water. Note that this definition does not impose a minimum nor maximum to the Hounsfield scale.

This study refers to CT acquisitions of metallic materials submerged in a water phantom. These CT images have been acquired with two different ranges of the Hounsfiled scale: the CHU and the EHU range, respectively. Both ranges are defined by imposing restrictions to the Hounsfield scale (1), i. e. by limiting it to particular upper and lower HU values. A CT image acquired at CHU range uses 12 bit per pixel to represent a HU interval from $HU_{\text{min}} = -1024$ HU to $HU_{\text{max}} = 3071$ HU. Consequently, at CHU all values above the maximum will be in saturation and represented as a constant value of $HU_{\text{max}} = 3071$ HU [17]. In contrast, the EHU range reflects a 10 times broader HU interval of $[-10240, 30710]$ HU. Choosing this interval allows to differentiate between the high-density metals and its surroundings [16]. However, metals may cause artifacts on CT images at both HU ranges which complicates a proper geometric delineation of the metallic objects and the structures nearby.

A Siemens Somatom Definition Flash Dual Source CT scanner providing the above mentioned HU ranges was used. Maximum tube energy of 100 kV and 140 kV was available. The CT scanner provided metal artifact reduction (MAR) algorithms developed to improve image quality and RT treatment planning [17, 18]. CT images of the following test objects have been acquired: (i) an IPG, (ii) a titanium disc ($D = 46.7$ mm, $\Delta d = 0.6$ mm), (iii) a copper disc ($D = 46.2$ mm, $\Delta d = 0.6$ mm) and (iv) an open cut empty titanium IPG case ($l = 20.1$ mm, $b = 47.7$ mm, $h = 11.3$ mm, $d = 0.6$ mm). Figure 1 sketches the scanning volume which was composed of a water filled acrylic tank. A water equivalent solid state slab phantom, made of a white polystyrene material (RW3), was positioned in the tank. The test objects were embedded and fixed between two RW3 slabs, which were separated by two thin separators positioned at the edges of the slab phantom. Several RW3 slabs were positioned under the object to account for any backscattering by the patient table.

Computerized tomography scans were acquired using an extremity protocol. The average X-ray energy used for the scans was 100 kV_p at 144 mA along with slice thickness

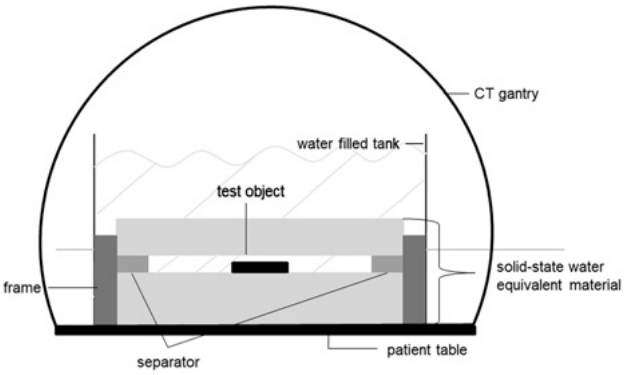

Figure 1: A simplified sketch of the set-up for the CT acquisition of the metallic test objects. The gap between the test object and the separator is filled with water.

of $\Delta s = 0.6$ mm in helical mode. The out-plane z-resolution was equal to the slice thickness Δs. The IPG was scanned with MAR in the CHU and in the EHU scales and without MAR in EHU. Scanning of the copper, titanium discs and the titanium made IPG case followed the same procedure. They were placed in the phantom and scanned in one pass. For the analysis of HU values the Fiji software was used [19]. The same circle shaped region of interest (ROI, size 77 pixel) was manually selected in CHU and EHU images to obtain data from identical volumes. The diameter D and thickness Δd of the discs were calculated on CT-images at both HU ranges. The results were compared to the real values.

3 Results

Figure 2 plots the impact of different HU ranges on the diameter and the thickness of the discs made of titanium

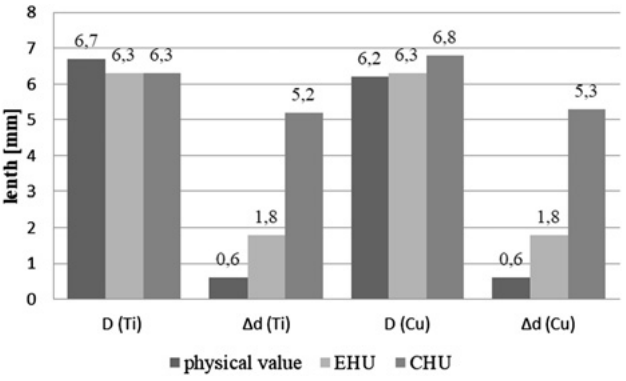

Figure 2: Comparison of diameter (D) and thickness (Δd) of a titanium and copper discs, measured on CT images taken at the CHU and the EHU range, both with MAR. In order to reuse the vertical scale, 40 mm are subtracted from each diameter value before plotting, e. g. the titanium disc diameter at EHU is $D = (40 + 6,3)$ mm.

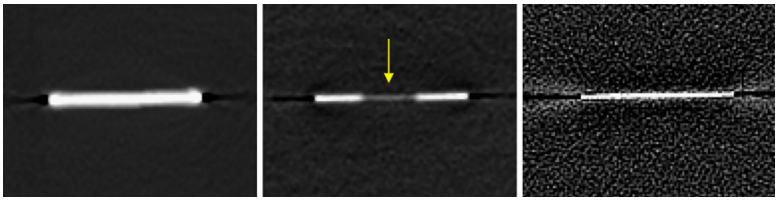

Figure 3: CT-image slice of a copper disc. CHU with MAR (left), EHU with MAR (middle), where a yellow arrow indicates effects due to MAR, and EHU without MAR (right).

and copper in comparison to real values. The diameter is in good agreement with the physical measurement in both acquisition types and for both objects. The real thickness of the discs was $\Delta d = 0.6$ mm, which was reconstructed many times larger (factor 9 for both materials) using the CHU range. Also when using the EHU range the thickness of the discs was overestimated, although not as much as with the CHU range.

Hounsfield values of the metallic test objects at a conventional and extended HU range, with and without MAR are listed in Table 1. The titanium IPG case is investigated in more detail: a) the upper lid and b) the curved ring connecting the upper with the lower lid as showed in Fig. 5. HU values in the EHU range with MAR show lower results as compared to the HU values in CHU range. This effect is observed for all objects. In contrast, the HU values in EHU without MAR represent higher values as compared to the values in the CHU range. In the conventional range, the HU value of the titanium and copper discs are 1571 HU and 3066 HU, respectively. The copper disc shows a two times higher HU value as compared to the titanium. This relation can be observed in the EHU range as well both with and without MAR.

Table 1: HU values of metallic objects determined at CHU and EHU range with and without MAR. (ROI size is 77 pixel). The physical densities of objects used are no exactly known, thus, we do not include a quantitative comparison of measured HU avlues versus object densities.

Object	CHU with MAR mean ± σ	EHU with MAR mean ± σ	EHU w/o MAR mean ± σ
titanium disc	1571 ± 88	1140 ± 5	2160 ± 31
titanium IPG, a)	1200 ± 145	1080 ± 9	1820 ± 45
titanium IPG, b)	3071 ± 1	1850 ± 30	4010 ± 30
copper disc	3066 ± 12	2390 ± 36	4130 ± 115

Figure 3 displays a CT slice of the copper disc acquired at CHU and EHU with and without MAR. The copper disc appears thicker in CHU compared to the other scans, which supports the results in Fig. 2. However, the CT image in CHU range with MAR displays a homogeneous representation of the test object, while the image in EHU range with MAR shows inhomogeneities (middle, see arrow). In contrast, the CT image in EHU without MAR displays a more accurate reconstruction of the disc thickness and a more homogeneous material representation. However, a comparison of a cross-sectional profile through the CT images of the test objects in EHU interval with and without MAR, underlines that both CT reconstructions are inhomogeneous (Fig. 4). The HU distribution in EHU range without MAR shows a quadratic progression, while with MAR it displays an irregular behaviour. Nonetheless, the signal to noise ratio in EHU range without MAR appears worse compared to the scans in both acquisition types with MAR. The highest HU values were always determined at the edges of the metallic test objects for all materials in all acquisition types, which were independent of MAR usage (Fig. 4 and Fig. 5). The HU values of the titanium IPG case show inhomogeneities in both HU ranges. The lids shows HU values almost 40 % lower as compared to the ring (see Fig. 5).

Figure 6 presents different cross-sectional CT images through an IPG. The first two image rows show the inner

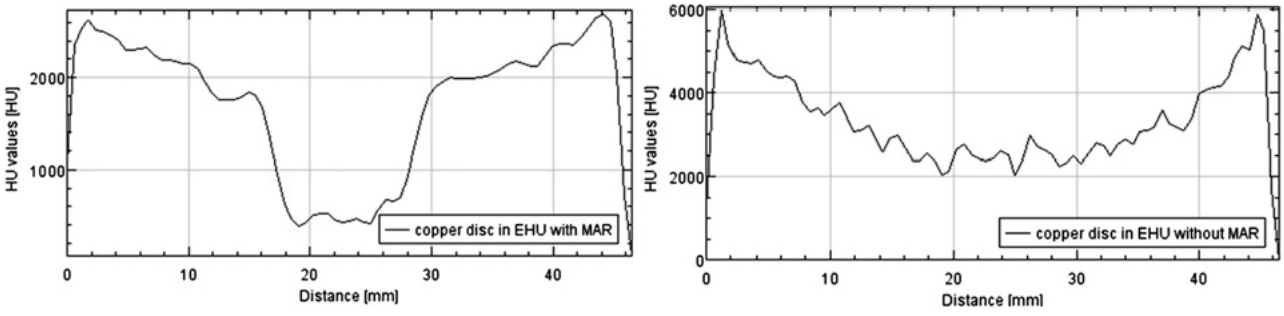

Figure 4: Cross-section profile through the CT scan of a copper disc in EHU with MAR (left) and without MAR (right).

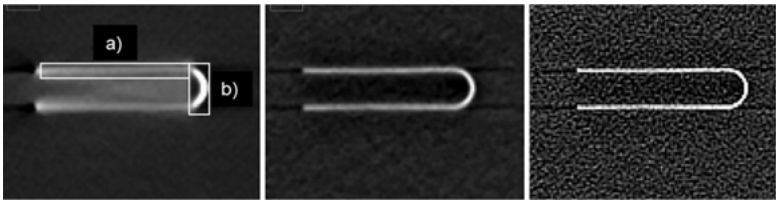

Figure 5: CT slice of an empty titanium IPG case lid a) and ring b). CHU with MAR (left), EHU with MAR (middle), and EHU without MAR (right).

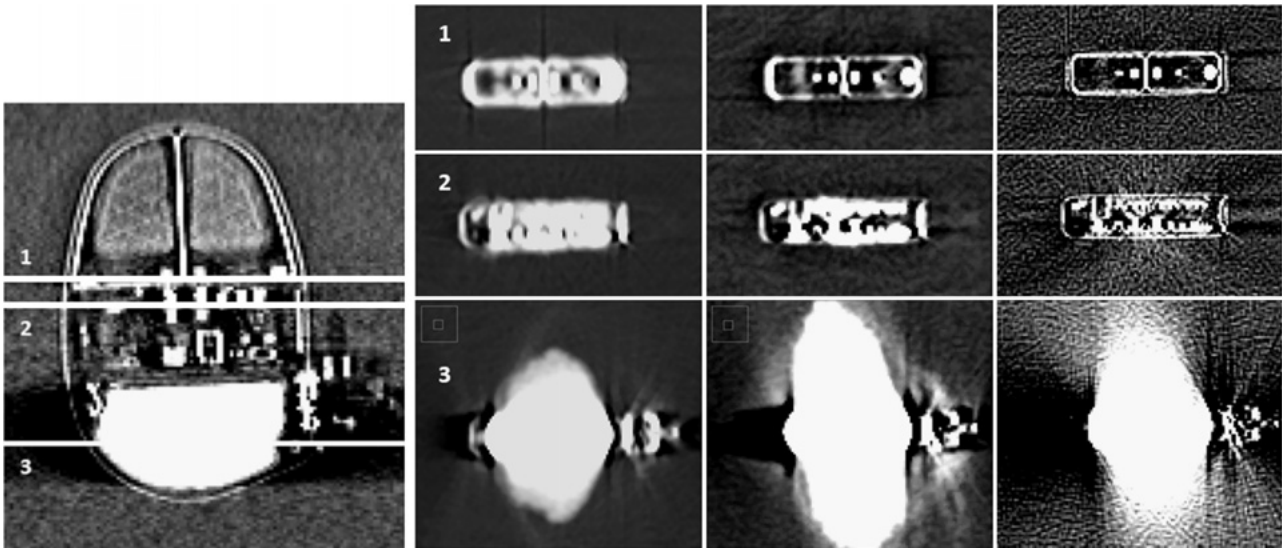

Figure 6: On the left the coronal view of the IPG is shown. The horizontal lines, labeled with 1, 2, 3, represent the position of the CT slices shown to the right of the coronal view. The CT slices are arranged in three columns corresponding to the CHU range (left column), the EHU range with MAR (middle column) and EHU range without MAR (right column).

part containing the electronics of an IPG. The contours of the different components are not well-defined on CT scans in the CHU range (left) as compared to the scans in the EHU range. HU value distribution in the inner part of the IPG is mostly set to the maximum achievable HU value. The air-filled regions within the IPG are distinguishable. In comparison to the CT images in EHU range with MAR, the images in EHU range without MAR enables a more accurate definition of the different components such as the IPG case and the particular electronics. However, streaking artifacts are clearly visible in all acquisition types. This artifact is dominantly visible at slices through the entrance and the exit of the IPG (last row in Fig. 6).

4 Discussion and conclusions

The depicted thickness Δd of the titanium and copper discs showed significant differences in the two CT acquisition types. The EHU range allowed for a more accurate geometric representation of the objects, merely an overestimation of the disc thickness by a factor of three was found. However, this discrepancy can be tracked back to the z-resolution being 0.6 mm/px, which could cause partial volume effects in image reconstruction for metallic discs of 0.6 mm thickness. It should be noted however, that a nine times larger thickness of the objects was determined in CHU range. Among others, the geometric accuracy in image reconstruction is essential for accurate dose calculation in RT TPS. Therefore, imaging in the EHU range shows more satisfying results in order to achieve RT goals.

As shown in Tab. 1 in CHU range the HU value of titanium was determined as $HU = (1571 \pm 88)$ HU and copper with a two times higher HU value of $HU = (3066 \pm 12)$ HU. The HU value of copper is two times higher than the HU value of titanium in the EHU range as well, so that the relation of a factor of two remains constant (as it should be due to the definition of the HU values). It can be assumed that in the CHU range, copper with a HU value of $HU = (3066 \pm 12)$ HU saturates at the maximum achievable HU value. Therefore, a higher HU value was expected in EHU range. Contrary to expectations, the HU values in the EHU range with MAR were even lower than the HU values in the CHU range. In addition, the HU distribution of

the test objects was inhomogeneous on the CT scans. This is considered as an effect of MAR algorithm, which suppresses streaking artifacts by applying filters but also affects the quantification of the HU values. After switching off the MAR mode the HU values increased for all test objects. Metal artifact reduction on CT images is helpful for diagnostic purposes and geometric accuracy but falsifies the quantified HU values of high-density materials. This could influence the accuracy of dose calculation in RT TPS as well. Therefore, for RT the CT acquisition in EHU range without MAR provides more reliable density quantification as compared to the other modes.

In 2016, a study by Gossman [20] recommended to include the electronics of AIMDs in the TPS calculation matrix in order to achieve a more accurate dose calculation and to account for AIMD dose monitoring to guarantee device safety. As can be seen in Fig. 6 the inner structures of an AIMD were well-defined on CT images in the EHU range without using MAR. There are still huge streaking artifacts on the outer boarders of the IPG case, which requires improvement. Nevertheless, for the purposes of radiotherapy CT scanning using extended EHU range appears adequate to properly represent metallic objects. However, the current setup might not be appropriate for dental implants as the phantom is not designed for jaw environments.

In conclusion, the EHU range better reproduces HU values of high-density materials thus rendering itself appropriate for the purpose of dose calculations in radiotherapy treatments. Image resolution, especially in z-direction, and artifacts degrade the geometrical truthfulness and accuracy. Metallic artifact reduction algorithms underestimates HU values calling for an additional detailed investigation. The findings of this study open up future investigations of malfunctions of active implants due to radiation in radiotherapy.

Acknowledgment: We would like to thank L. Lüdemann, University Hospital Essen, Germany, for supporting this study.

Funding: This study is supported by the Federal Ministry for Economic Affairs and Energy on the basis of a decision by the German Bundestag, grant no. ZF4205702AW6.

References

1. Robert Koch Institute. Beitraege zur gesundheutsberichterstattung des bundes. krebs in deutschland, 2016. URL http://www.rki.de/Krebs/DE/Content/Publikationen. last visited on 2017-09-26.
2. Krebsgesellschaft. Strahlentherapie, 2017. URL https://www.krebsgesellschaft.de/onko-internetportal/basis-informationen-krebs/therapieformen/strahlentherapie-bei-krebs.html. last visited on 2017-09-26.
3. B. Gauter-Fleckenstein, C.W. Israel, M. Dorenkamp, J. Dunst, M. Roser, R. Schimpf, V. Steil, J. Schäfer, U. Höller, and F. Wenz. Degro/dgk guideline for radiotherapy in patients with cardiac implantable electronic devices. *Strahlentherapie Onkologie*, 191: 393–404, March 2015.
4. T. Zaremba. *Radiotherapy in Patients with Pacemakers and Implantable Cardioverter-Defibrillators*. PhD thesis, Aalborg University, 2015.
5. J.I. Prisciandaro, A. Makkar, C.J. Fox, J.A. Hayman, F. Horwood, L. Pelosi, and J.M. Moran. Dosimetric review of cardiac implantable electronic device patients receiving radiotherapy. *Journal of Applied Clinical Medical Physics*, 16: 1–8, October 2014.
6. C.W. Hurkmans, E. Scheepers, B.G.F. Springorum, and H. Uiterwaal. Influence of radiotherapy on the latest generation of implantable cardioverter-defibrillator. *Int. J. Radiation Oncology Biol. Phys.*, 63 (1): 282–289, April 2005.
7. C.W. Hurkmans, E. Scheepers, B.G.F. Springorum, and H. Uiterwaal. Influence of radiotherapy on the latest generation of pacemakers. *Radiotherapy and Oncology*, 76 (1): 93–98, April 2005.
8. J.R. Marbach, M.R. Sontag, J. Van Dyk, and A.B. Wolbarst. Management of radiation oncology patients with implanted cardiac pacemakers: Report of aapm task group no. 34. *Medical Physics*, 21 (1): 85–90, January 1994.
9. C.W. Hurkmans, J.L. Knegjens, B.S. Oei, Ad.J.J Maas, G.J. Uiterwaal, A.J. Van der Borden, M.J. Ploegmakers, and L. Van Erven. Management of radiation oncology patents with a pacemaker or icd: a new comprehensive practical guideline in the netherlands. dutch society of radiotherapy and oncology (nvro). *Radiation Oncology*, 7 (198): 1–10, November 2012.
10. A. Bourgouin, N. Varfalvy, and L. Archambault. Estimating and reducing dose received by cardiac devices for patients undergoing radiotherapy. *Journal of Applied Clinical Medical Physics*, 16 (6): 411–420, August 2015.
11. J.Y. Huang, D.S. Followill, X.A. Wang, and S.f. Kry. Accuracy and sources of error out-of-field dose calculations by commercial treatment planning system for intensity-modulated radiation therapy treatments. *Journal of Applied Clinical Medical Physics*, 14 (2): 4139, 2015.
12. R.M. Howell, S.B. Scarboto, S.F. Kry, and D.Z. Yaldo. Accuracy of out-of-field dose calculations by a commercial treatment planning system. *Physics in Medicine and Biology*, 55 (23): 6999–7008, 2010.
13. T. Kairn, S.B. Crowe, J. Kenny, J. Mitchell, D. Burke, M. Schlect, and J.V. Trapp. Dosimetric effects of a high-density spinal implant. *Journal of Physics: Conference Series, 7th International Conference on 3D Radiation Dosimetry*, 444: 1–4, January 2008.
14. J.P. Mullins, M.P. Grams, M.G. Herman, D.H. Brinkmann, and J.A. Antolak. Treatment planning for metals using an extended ct number scale. *Journal of Applied Clinical Medical Physics*, 17 (6): 179–188, August 2016.
15. M.S. Gossman, A.R. Graves-Calhoun, and J.D. Wilkinson. Establishing radiation therapy treatment planning effects involving implantable pacemakers and implantable

cardioverter-defibrillator. *Journal of Applied Clinical Medical Physics*, 11 (1): 33–45, August 2009.
16. C. Coolens and P.J. Childs. Calibration of ct Hounsfield units for radiotherapy treatment planning of patients with metallic hip prostheses: the use of the extended ct-scale. *Physics in Medicine and Biology*, 48: 1591–1603, May 2003.
17. G. Hilgers, T. Nuver, and A. Minken. The ct number accuracy of a novel commercial metal artifact reduction algorithm for large orthopedic implants. *Journal of Applied Clinical Medical Physics*, 15 (1): 274–278, September 2014.
18. K.M. Andersson, A. Ahnesjö, and C.V. Dahlgren. Evaluation of a metal artifact reduction algorithm in ct studies used for proton radiotherapy treatment planning. *Journal of Applied Clinical Medical Physics*, 15 (5): 112–119, May 2014.
19. J. Schindelin, I. Arganda-Carreras, and E. Frise. Fiji: an open-source platform for biological-image analysis. *Nature methods*, 9 (7): 676–682, 2012.
20. M.S. Gossman. Clinical Concerns and Strategies in Radiation Oncology, *Aspects of Pacemakers-Functions and Interactions in Cardiac and Non-cardiac Indications*. InTech, 2016.

Bionotes

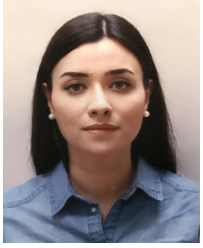

Zehra Ese
MR:comp GmbH, Buschgrundstraße 23, 45894 Gelsenkirchen, Germany; and Laboratory for General and Theoretical Electrical Engineering (ATE), Faculty of Engineering, University of Duisburg-Essen, Bismarckstrasse 81, 47048 Duisburg, Germany; and Faculty of Electrical Engineering and Applied Natural Sciences, Westphalian University, Campus Gelsenkirchen, Neidenburger Strasse 43, 45897 Gelsenkirchen, Germany
ese@mrcomp.com

Zehra Ese received in 2013 a B. Sc. degree in Physical Engineering from the Westphalian University of Applied Sciences Gelsenkirchen, Bocholt, Recklinghausen, and in 2015 a M.Sc. degree in Biomedical Engineering from the Ruprecht-Karls Heidelberg University, respectively. She is currently working toward a PhD degree in electrical engineering at the University of Duisburg-Essen in cooperation with the Westphalian University of Applied Sciences Gelsenkirchen, Bocholt, Recklinghausen. Zehra Ese is also involved as a research associate at the MR:comp GmbH. Her general research interest includes biomedical engineering, medical physics, radiation physics and computational modelling. Her recent research investigates the analysis of interactions of ionizing radiation and electronics in medical applications.

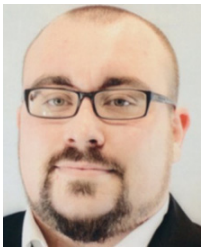

Marcel Kressmann
MR:comp GmbH, Buschgrundstraße 23, 45894 Gelsenkirchen, Germany
kressmann@mrcomp.com

Marcel Kressmann received in 2013 a B. Sc. and in 2017 a M.Sc. degree in Medical Engineering from the Westphalian University of Applied Sciences Gelsenkirchen, Bocholt, Recklinghausen, respectively. From 2011 to 2014, he was involved as a student associate and continued as a testing engineer at the MR:comp GmbH until September 2017. Currently, he is a technical support engineer at the stryker GmbH & Co.KG.

Jakob Kreutner
MR:comp GmbH, Buschgrundstraße 23, 45894 Gelsenkirchen, Germany; and MRI-STaR – Magnetic Resonance Institute for Safety, Technology and Research GmbH, Buschgrundstraße 23, 45894 Gelsenkirchen, Germany
kreutner@mrcomp.com

Jakob Kreutner studied physics at the University of Würzburg, Germany. After his diploma in 2009 he joined the Research Center for Magnetic Resonance Bavaria e. V. in Würzburg. During that time his work was focused on quantitative characterization of bone microstructure using magnetic resonance imaging. In 2015 he joined the research department at MR:comp GmbH. His research is focusing on MR safety and compatibility for medical devices. Since 2016 he is leading the research department also at MRI-STaR, a newly founded company addressing research related testing of devices.

Gregor Schaefers
MR:comp GmbH, Buschgrundstraße 23, 45894 Gelsenkirchen, Germany; and MRI-STaR – Magnetic Resonance Institute for Safety, Technology and Research GmbH, Buschgrundstraße 23, 45894 Gelsenkirchen, Germany
schaefers@mrcomp.com

Gregor Schaefers obtained his Dipl.-Ing. (FH) degree in medical engineering from the University of Applied Sciences Fachhochschule Gelsenkirchen, Germany, in 2001 and received the Erich-Mueller-Award for the best thesis of the year. He is the founder, shareholder, and managing director of MR:comp GmbH (www.mrcomp.com), a specialized test laboratory with a team of over 55 employees working worldwide on MR safety and compatibility testing of medical devices following ISO 17025 accreditation. He is founder, shareholder, and managing director of the MRI-STaR – Magnetic Resonance Institute for Safety, Technology and Research GmbH working in the field of MR safety and compatibility development and optimization of

experimental and numerical MR testing methods, RF coil safety, MR sequence programming, MR workflow optimization, international MR Safety Expert (MRSE) and MR Safety Specialist (MRSS) seminars and partner of www.MRI-tec.com ONE-STOP SHOP for MR Safe and MR Conditional devices. Gregor Schaefers is member of DIN - German Institute for Standardization, ISO, and IEC as well as ASTM standardization committees, and he is convener of IEC TC62 working group WG45 for IEC 62570. Furthermore, Gregor Schaefers is author of scientific and technical congress as well as journal publications and book chapters with respect to MR safety and compatibility.

Daniel Erni
Laboratory for General and Theoretical Electrical Engineering (ATE), Faculty of Engineering, University of Duisburg-Essen and CENIDE – Center of Nanointegration Duisburg-Essen, Bismarckstrasse 81, 47048 Duisburg, Germany
daniel.erni@uni-due.de

Daniel Erni is a full professor for General and Theoretical Electrical Engineering at the University of Duisburg-Essen, Germany. After an apprenticeship as an electrician and mechanic he received his two degrees in electrical engineering from HSR Rapperswil and ETH Zürich in 1986 and 1990, respectively, and a PhD degree in laser physics from ETH Zurich in 1996. He has co-authored and authored over 400 scientific publications. His current research interests include optical interconnects, nanophotonics, plasmonics, optical and electromagnetic metamaterials, RF, mm-wave and THz engineering, biomedical engineering, marine electromagnetics, computational electromagnetics, multiscale and multiphysics modeling, numerical structural optimization, and science and technology studies (STS).

Waldemar Zylka
Faculty of Electrical Engineering and Applied Natural Sciences, Westphalian University, Campus Gelsenkirchen, Neidenburger Strasse 43, 45897 Gelsenkirchen, Germany
waldemar.zylka@w-hs.de

Waldemar Zylka is a full professor of Physics and Medical Engineering at the Westphalian University, Campus Gelsenkirchen, Germany. He received the degree Diplom-Physiker and in 1993 the Doctor degree in theoretical Physics, both from the Albert-Ludwigs-University Freiburg i. Br., Germany. He has co-/authored numerous scientific publications and patents. He is serving as member of program committees and as reviewer for international meetings and journals. His current research focuses are system biology, multi-scale modelling, and computational electromagnetics particularly for medical imaging modalities.